Chromium deposition on ordered alumina films: An x-ray photoelectron spectroscopy study of the interaction with oxygen

M. Eriksson, J. Sainio, and J. Lahtinen[a)]
Laboratory of Physics, Helsinki University of Technology, P.O. Box 1100, 02015 HUT, Finland

We have studied metallic and oxidized chromium layers on thin ordered alumina films grown on a NiAl(110) substrate using x-ray photoelectron spectroscopy. The interaction between the chromium layers and the substrate has been characterized after deposition at room temperature and after oxidation at 300 and 700 K. Our results indicate partial oxidation of the deposited chromium with the fraction of oxidized Cr decreasing with increasing Cr coverage. Oxidation of the chromium layers at room temperature using O_2 results in Cr^{3+} species on the surface. These oxidized chromium species can be reduced by heating the sample to 700 K for 5 minutes. Oxidation at 700 K results in chromium species that cannot be thermally reduced. Our results do not indicate formation of Cr^{6+} species although such are present in impregnated catalysts. © *2002 American Institute of Physics.* [DOI: 10.1063/1.1434954]

I. INTRODUCTION

Chromium oxide supported on aluminum oxide is a widely used catalyst, e.g., in polymerization of ethylene, dehydrogenation of paraffins, and selective oxidation of alcohols.[1,2] Supported chromium oxide catalysts investigated by XPS has been the subject of numerous studies.[1–5]

The porous and insulating support materials used in catalysts limit the amount of information obtainable on the surface of real catalysts. Proper oxidation of the NiAl(110) alloy single crystal results in a thin, well-ordered alumina film with a surface structure reminiscent of bulk γ-Al_2O_3.[6–8] The alumina film formed on NiAl(110) is thin enough to allow electron and ion spectroscopies to be used without the charging problems normally associated with insulating samples. Easy heating and thermal equilibrium throughout the sample are ensured by the metallic properties of the NiAl alloy.

Deposition of several noble and transition metals on the Al_2O_3/NiAl(110) surface have been studied (see Ref. 9 for a review). The growth of the metal layer exhibit formation of 3D particles close to Volmer–Weber (VW) fashion in most of the systems, like V,[10] Rh,[11] Co, and Pd.[12,13] Platinum has received the most intense attention and it has been found to grow two dimensionally with the Pt particles modifying the structure of the support.[14–17] There is only one study made with chromium on alumina on NiAl(100). In this study the oxide is present as thin ordered stripes on the alloy crystal. The evaporated Cr formed small metallic clusters with a mean size of 3 nm.[18] Ultrathin Cr films on TiO_2(110) have also been studied previously.[19] The results indicate quasi-two-dimensional growth of Cr on the surface resulting in oxidation of Cr species at the interface. When thicker Cr layers were formed also metallic Cr was detected.

In this work chromium was thermally deposited onto the thin alumina film in ultrahigh vacuum (UHV). Chromium oxide was formed by exposing the thin chromium film to oxygen in vacuum. The chromium and chromium oxide films were characterized using x-ray photoelectron spectroscopy (XPS). We focused our attention on the initial interaction between the oxygen terminated alumina support and the deposited chromium. We also investigated the interaction between chromium and oxygen at low O_2 exposures.

II. EXPERIMENT

The experiments reported in this paper were performed in a stainless steel UHV chamber with a base pressure of 2×10^{-10} Torr. The sample cleanliness was measured with Auger-electron spectroscopy (AES) using a double pass cylindrical mirror analyzer (DPCMA) with an integral electron gun. The XP and AE spectra were both recorded using the DPCMA with a pass energy of 50 eV. Both Al$K\alpha$ and Mg$K\alpha$ radiation was used in the XPS experiments and the binding energies were referenced to the Ni $2p_{3/2}$ and Ni $3p$ peaks at 852.7 eV and 66.5 eV, respectively.[20]

Our NiAl(110) sample had a diameter of roughly 10 mm and a thickness of a few millimeters. Connection of the sample to the sample holder was accomplished through tantalum wires that passed through four holes drilled into the sample. These wires were also used for sample heating. The temperature of the sample was monitored by a chromel–alumel thermocouple that was spot-welded to the back of the sample.

Cleaning of the sample was performed using 3 keV Ar$^+$ ion sputtering with 25 μA emission for 60 minutes at room temperature. Sputtering was continued at 700 K for 30 minutes. Subsequent annealing at 1150 K for 45–60 minutes gave a sharp (1×1) LEED pattern of the NiAl(110) surface.

Formation of the thin, well-ordered alumina film was performed by exposing the clean and annealed NiAl(110) crystal to 3600 L ($1\,L = 10^{-6}$ Torr s) of O_2 at 550 K followed by annealing for 3 minutes at 1150 K. More informa-

---
[a)]Author to whom correspondence should be addressed. Electronic mail: jouko.lahtinen@hut.fi
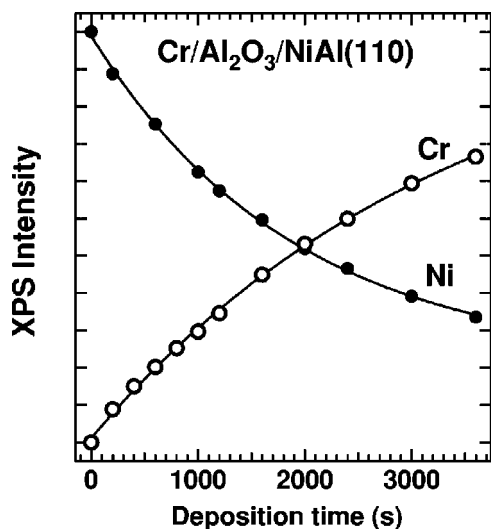
FIG. 1. XS−t plot for prolonged chromium deposition onto Al_2O_3/NiAl(110). The lack of break points in the Ni $2p_{3/2}$ signal and in the Cr $2p$ signal indicates three-dimensional growth.

tion on this procedure has been given elsewhere.[6–8,12,21] The rather complicated LEED pattern associated with the ordered alumina film[7] was used as a measure of the correct surface structure.

Chromia–alumina model systems were prepared through vapor deposition of thermally evaporated metallic Cr onto the well-ordered Al_2O_3/NiAl(110) surface. The chromium evaporator was built from a tungsten filament basket that was holding an aluminum oxide crucible. Chromium lump with a bulk purity of >99.0% was used. The evaporator was typically driven by 35 A and 7.5 V. A water cooled cylindrical pipe enclosed the evaporator to keep the background pressure in the UHV chamber below 2×10^{-9} Torr during operation of the evaporator. The chromium evaporator produced constant vapor flux in all the experiments providing the possibility to control the layer growth by the evaporation time and current.

III. RESULTS AND DISCUSSION

A. Deposition of chromium on the surface

The experiments were started by deposition of Cr onto the Al_2O_3/NiAl(110) surface. The growth of Cr layer was followed by recording both the XPS $2p$ signals and the AES KLL signals of Cr and Ni. The XPS intensity versus time has been plotted in Fig. 1. The information provided by the XS−t plot indicates some kind of three-dimensional growth since there is no breaks visible in the XS−t plot for neither Ni $2p_{3/2}$ nor Cr $2p$. The data points fall nicely on exponential curves, which indicates growth in simultaneous monolayers (SM)[22] or in two-dimensional islands (2DI).[23,24] The SM growth occurs when the diffusion along both the substrate and the adsorbate surface is minimal and the film is formed from several one atom high layers. In the 2DI mode the layer grows in layer-by-layer fashion forming 2D islands, but before the completion of the layer when a critical coverage (15–85%) is reached the formation of the next layer begins.[23] The 2DI mode can be regarded as a intermediate

type of film growth between SM and layer-by-layer growth where the diffusion along the surface defines the exact growth type. Fitting of an exponential curve to the XS−t plot gave a nominal deposition rate of $(3.4 \pm 0.2) \times 10^{12}$ Cr/cm^{2}s.

Volmer–Weber (VW) growth has been reported for most metal deposits investigated on thin alumina films at various deposition temperatures,[9] and surface free energy arguments strongly favor VW growth of metal layers on thin alumina films. However, the rapid increase in the adsorbate signal indicates that the Cr islands cover a substantial part of the surface and the growth is not characteristic of true VW growth. First hand information obtainable via STM investigations would be needed to confirm our suspicion that kinetic limitations at room temperature lead to 2DI growth of Cr on Al_2O_3/NiAl(110).

B. Interaction of deposited Cr and the Al_2O_3 surface

We deposited chromium onto the surface at five different nominal coverages ranging from 3.4×10^{14} to 4.1×10^{15} Cr atoms/cm^2 as determined from the deposition rate using 100, 200, 400, 600, and 1200 s deposition time. For reference, the topmost oxygen layer of the thin alumina film has an oxygen atom density of 1.27×10^{15} atoms/cm^2.[7] If this number is used as a reference for one monolayer the coverages are between 0.27 and 3.2 ML. The coverages presented here are estimates only since no independent method was used for the calibration of the vapor flux.

The interaction between the chromium particles and the Al_2O_3/NiAl(110) substrate was studied by recording the Cr $2p$ line after Cr deposition. The Cr $2p$ XP spectra for the different chromium coverages are shown in Fig. 2. The analysis of the Cr $2p$ spectra were done using Gaussian peaks after Tougaard background subtraction.[25–27] Doublet peaks were fitted for all chromium species. Based on experiments with alumina supported chromium catalysts presented in the literature, we used binding energies for chromium according to Table I.

During our analysis the binding energies were kept constant within ± 0.3 eV, the doublet separation of the Cr $2p_{3/2}$ and Cr $2p_{1/2}$ peaks within ± 0.1 eV and the full-width at half maximum (FWHM) within ± 0.3 eV from the values presented in Table I. The Cr $2p_{3/2}$/Cr $2p_{1/2}$ intensity ratio was set to 0.55 ± 0.03.[5] A shake-up satellite line was added 4.1 eV above the Cr^{3+} peak according to previous studies. The intensity of the satellite peak was kept at 0.32 ± 0.03 (Ref. 5) compared to that of the Cr^{3+} main line. We were able to confirm this value from our own investigations following oxidation of the deposited chromium (see below). No satellite structures were used with the other Cr components.

The decompositions of selected Cr spectra are shown in Fig. 2. A component that was assigned to metallic chromium located at 574.0 eV is present for all Cr coverages. There is also a component visible at 576.7 eV, which was attributed to Cr^{3+}. A satisfactory decomposition of the spectra requires introduction of a peak at approximately 575.2 eV. Until further evidence has been presented we assign this feature to Cr^{2+}. The nonconclusive assignment is needed because
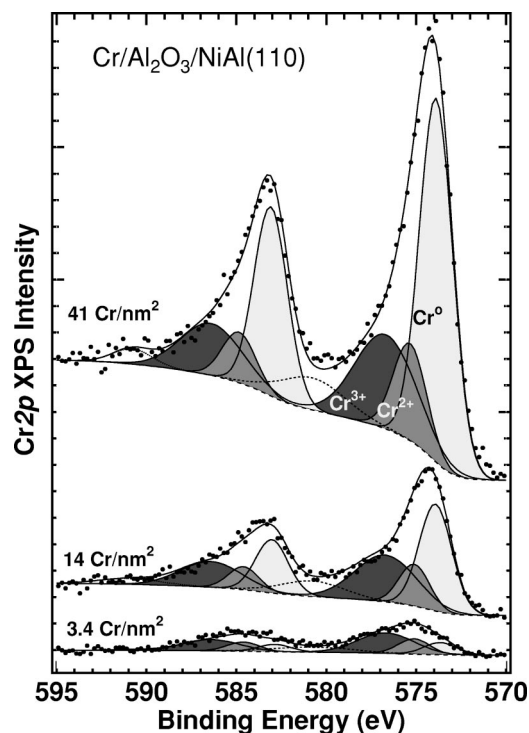
FIG. 2. Cr $2p$ XP spectra of selected amounts of chromium deposited onto the Al_2O_3 /NiAl(110) surface. Decomposition has been done using Gaussian peaks following Tougaard background subtraction. The shift of the peak position towards lower binding energies indicates increased amounts of metallic Cr.

Cr^{4+} has been reported to have a binding energy equal[30] or about 0.5 eV below of the binding energy of Cr^{3+}.[31]

For the lowest coverage, the Cr $2p_{3/2}$ peak is located at around 576 eV and cannot be interpreted as mainly metallic chromium. Our results indicate that the interaction between the first chromium layer and the oxygen terminated alumina film results in chromium oxide for low Cr coverages. The binding energy of Cr $2p_{3/2}$ shifts towards metallic chromium with Cr coverage but in every case three components were needed to reproduce the measured spectra. This indicates formation of larger Cr clusters.

It has been proposed that the occurrence of final state effects[32,33] for small conducting particles on insulators could explain the shift towards higher binding energies for low coverages. However, the conductivity through the thin alumina film is sufficient to effectively reduce or even eliminate final state effects.[34] Finding the Cr^{2+} component also at higher Cr coverages, where larger Cr clusters were expected, at almost constant concentration, as can be seen in Fig. 3, is an evidence that the +2 state exists in the initial interaction between Cr and Al_2O_3 /NiAl(110).

TABLE I. Parameters for the Cr $2p$ XPS peak.

Cr species	BE (eV)	FWHM (eV)	$\delta(2p_{3/2}-2p_{1/2})$ (eV)	References
Cr^0	574.0	2.2	9.1	3, 5, 28
Cr^{2+}	575.3	2.2	9.5	5, 29
Cr^{3+}	576.7	3.8	9.7	1–3, 5
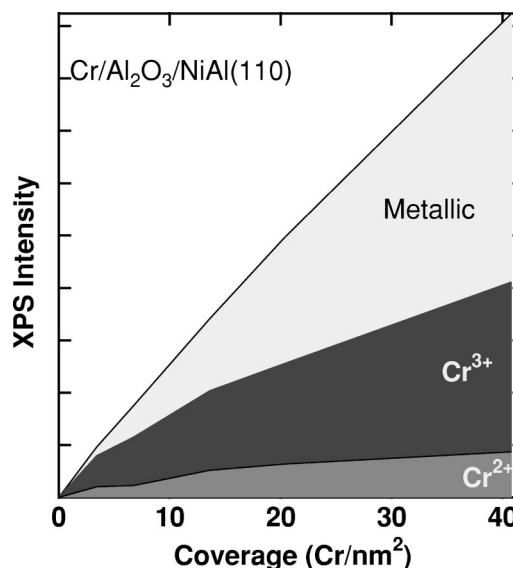
FIG. 3. Evolution of the different oxidation states with chromium coverage during Cr deposition on Al_2O_3 /NiAl(110).

Provided that heterogeneous nucleation prevails at room temperature, we could expect decoration of defects on the surface. Depending on the type of defect acting as a nucleation center we then could see different oxidation states at these defects. In the present study this could explain the occurrence of two oxidation states, namely +2 and +3.

Part of the highly reactive Cr might be oxidized through reaction with residual molecules that contain oxygen present in the UHV chamber.[10] We do not, however, expect this to significantly change our interpretation of the $Cr–Al_2O_3$ /NiAl(110) interaction.

C. Interaction with ambient oxygen

Based on the rather constant amount of Cr^2+ species we can propose that these atoms reside at the alumina Cr interface. The initial increase can be attributed to the growth of Cr islands as they slowly fill the surface. As the thickness of the film grows, attenuation due to the second layer compensate the growth in the interface signal.

For vanadium deposited onto the thin alumina film[10] a cationic behavior of the deposit was found up to a coverage of around 0.1 ML, where 1 ML corresponds to the lattice constant of bulk vanadium. It was concluded that the oxidation state was below +3, but the oxidation state distribution could not be determined more precisely.[10]

Similar results have also been reported for Cr on TiO_2(110).[19] Contrary to the case of Cr/TiO_2 we did not observe any sign of reduction in the Al $2p$ peak for the Cr/Al_2O_3 model system. This shows that TiO_2 is more easily reducible than Al_2O_3 /NiAl(110), which makes the oxidation of Cr even more interesting.

Exposing the highly reactive chromium layers to oxygen at room temperature resulted in clear changes in the shape of the Cr $2p$ spectra. These changes were fully developed at oxygen exposures between 1 and 3 L. A dose of 20 L was used, however, to ensure complete oxidation of the chromium. An example of the Cr $2p$ line for oxidized chromium

FIG. 4. Cr $2p$ XPS spectra of (a) an oxidized and (b) subsequently heated CrO$_x$/Al$_2$O$_3$/NiAl(110) sample with a chromium coverage of 2.0 $\times 10^{15}$ atoms/cm^2. Heating the oxidized chromium reduces the chromium to an average oxidation state below +3.

TABLE II. Oxidation state distribution for Cr on a well-ordered alumina film. Our estimate for the error is ±5%.

(Cr/nm^2)	Cr^0 (%)	Cr^{2+} (%)	Cr^{3+} (%)
As deposited			
3.4	18	21	61
6.8	34	13	53
13.6	40	15	45
20.4	49	13	38
40.8	53	14	33
Oxidized and reduced			
3.4	13	19	68
6.8	19	21	60
13.6	33	17	50
20.4	36	20	44
40.8	41	14	45

Performing the oxidation at 700 K formed a Cr $2p$ peak similar to that after oxidation at room temperature. Subsequently holding the sample at 700 K for 5 minutes produced no change in the oxidation state of the chromium overlayer. Interestingly it can be concluded that chromium oxidized at room temperature is thermally reducible. Chromium oxide formed at 700 K, however, is not thermally reducible in the same fashion and shows no sign of thermal instability for temperatures below 900 K.

Introduction of oxidation states higher than +3 for the Cr $2p$ spectra of the oxidized Cr was not necessary to fully explain the spectra. In reports where chromia–alumina catalysts have been calcined, Cr^{6+} species have been identified using, e.g., XPS[1–5] and UV–vis spectrophotometry.[2] In this light it is surprising that we were unable to find any Cr species that could be assigned a +6 oxidation state. On the other hand, the methods of real catalyst preparation differ significantly from the evaporation method used in these experiments, e.g., OH groups not inherently present in UHV conditions are thought to play a vital role both in catalyst formation and activity.

IV. CONCLUSIONS

Chromium deposited by thermal evaporation onto an ordered Al$_2$O$_3$/NiAl(110) support shows an initial oxidation during deposition. Although no exact answer can be given for the oxidation state distribution because of the possible influence of final state effects it can safely be stated that Cr exhibits an average oxidation state between +1 and +3 for low coverages on Al$_2$O$_3$/NiAl(110). For higher chromium coverages a shift towards metallic behavior is noticed.

We were able to clearly identify metallic and Cr^{3+} species in the interaction with the oxygen terminated alumina film. However, an additional oxidation state was needed for decomposition of the Cr $2p$ spectra. It is likely that this component has an oxidation state +2.

Oxidation of the deposited chromium leaves only Cr^{3+} species on the surface. If the oxidation is performed at room temperature a subsequent heating to 700 K will reduce the chromium to an average oxidation state lower than +3. When the oxidation is performed at 700 K no thermal reduction of the formed Cr^{3+} could be detected below 900 K.

on Al$_2$O$_3$/NiAl(110) is shown in Fig. 4(a). Using chromium with an oxidation state of +3 and its satellites results for a satisfactory decomposition of the spectrum. By analyzing the Cr $2p$ emission from the oxidized chromium layers we were able to confirm the intensity ratio between the Cr^{3+} satellite and main peak to 0.32.

It seems unlikely that introduction of ambient oxygen would shift the deposited Cr from a +4 oxidation state to a lower +3 oxidation state. With some reservation we can thus ascribe the component at 575.1–575.3 eV to Cr^{2+}.

Oxidation gives the same result for all chromium coverages investigated in this paper. This indicates that the size of the Cr clusters are relatively small compared to the diffusion length of oxygen in Cr.

Subsequent heating of the oxidized sample to 700 K in UHV for 5 minutes reduced the chromium to an average oxidation state below +3 as shown in Fig. 4(b). The results from the decomposition of the Cr $2p$ peak for the thermally reduced chromia–alumina system in comparison to deposited Cr is presented in Table II. It is not possible to decompose the spectrum of the reduced Cr by two components, but an additional component between metallic Cr and Cr^{3+} is required. We notice that the amount of Cr^{2+} is almost the same before oxidation and after reduction while the amount of Cr^0 decreases and Cr^{3+} increases following the oxidation/reduction cycle.

No indications of oxidation states higher than $+3$ for chromium could be seen following the preparations and treatments applied here.

ACKNOWLEDGMENTS

[1] F. Cavani, M. Koutyrev, F. Trifir, A. Bartolini, D. Ghisletti, R. Iezzi, A. Santucci, and G. Del Piero, J. Catal. **158**, 236 (1996).

[2] A. Kytökivi, J. P. Jacobs, A. Hakuli, J. Meriläinen, and H. H. Brongersma, J. Catal. **162**, 190 (1996).

[3] Y. Okamoto, M. Fujii, T. Imanaka, and S. Teranishi, Bull. Chem. Soc. Jpn. **49**, 859 (1976).

[4] B. Grzybowka, J. Sloczyński, R. Grabowski, K. Wcisło, A. Kozłowska, J. Stoch, and J. Zieliński, J. Catal. **178**, 687 (1998).

[5] W. Grünert, E. S. Shpiro, R. Feldhaus, K. Anders, G. V. Antoshin, and Kh. M. Minachev, J. Catal. **100**, 138 (1986).

[6] M. Klimenkov, S. Nepijko, H. Kuhlenbeck, and H.-J. Freund, Surf. Sci. **385**, 66 (1997).

[7] R. M. Jaeger, H. Kuhlenbeck, H.-J. Freund, M. Wuttig, W. Hoffman, R. Franchy, and H. Ibach, Surf. Sci. **259**, 235 (1991).

[8] J. Libuda, F. Winkelmann, M. Bäumer, H.-J. Freund, Th. Bertrams, H. Neddermeyer, and K. Müller, Surf. Sci. **318**, 61 (1994).

[9] M. Bäumer and H.-J. Freund, Prog. Surf. Sci. **61**, 127 (1999).

[10] M. Bäumer, J. Beinder, and R. J. Madix, Surf. Sci. **432**, 189 (1999).

[11] M. Bäumer, M. Frank, J. Libuda, S. Stempel, and H.-J. Freund, Surf. Sci. **454–456**, 957 (2000).

[12] S. Andersson, P. A. Brühwiler, A. Sandell, M. Frank, J. Libuda, A. Giertz, B. Brean, A. J. Maxwell, M. Bäumer, H.-J. Freund, and N. Mårtensson, Surf. Sci. **442**, L946 (1999).

[13] M. Bäumer, M. Frank, M. Heemeier, R. Kühnemuth, S. Stempel, and H.-J. Freund, Surf. Sci. **454–456**, 957 (2000).

[14] Th. Bertrams, F. Winkelmann, Th. Uttich, H.-J. Freund, and H. Neddermeyer, Surf. Sci. **331–333**, 1515 (1995).

[15] S. A. Nepijko, M. Klimenkov, H. Kuhlenbeck, D. Zymlyanov, D. Herein, R. Schlögl, and H.-J. Freund, Surf. Sci. **412–413**, 192 (1998).

[16] J. Libuda, M. Bäumer, and H.-J. Freund, J. Vac. Sci. Technol. A **12**, 2259 (1994).

[17] S. A. Nepijko, M. Klimenkov, M. Adelt, H. Kuhlenbeck, R. Schlögl, and H.-J. Freund, Langmuir **15**, 5309 (1999).

[18] J. Méndez and H. Niehus, Appl. Surf. Sci. **142**, 152 (1999).

[19] J.-M. Pan, U. Diebold, L. Zhang, and T. E. Madey, Surf. Sci. **295**, 411 (1993).

[20] *Handbook of X-ray Photoelectron Spectroscopy*, edited by J. Chastain (Physical Electronics Inc., USA, 1992).

[21] H. Isern and G. R. Castro, Surf. Sci. **211–212**, 865 (1989).

[22] C. Argile and G. E. Rhead, Surf. Sci. Rep. **10**, 277 (1989).

[23] C. T. Campbell, Surf. Sci. Rep. **27**, 1 (1997).

[24] K. H. Ernst, A. Ludviksson, R. Zhang, J. Yoshihara, and C. T. Campbell, Phys. Rev. B **47**, 13782 (1993).

[25] M. P. Seah, Surf. Sci. **420**, 285 (1999).

[26] M. P. Seah, I. S. Gilmore, and S. J. Spencer, Surf. Sci. **461**, 1 (2000).

[27] SpXZeigR routines by J. J. Weimer can be found at http://lmass.uah.edu/software/

[28] V. Maurice, S. Cadot, and P. Marcus, Surf. Sci. **458**, 195 (2000).

[29] A. Maetaki, M. Yamamoto, H. Matsumoto, and K. Kishi, Surf. Sci. **445**, 80 (2000).

[30] A. Cimino, B. A. de Angelis, A. Luchetti, and O. Minelli, J. Catal. **45**, 316 (1976).

[31] I. Ikemoto, K. Ishii, S. Kinoshita, H. Kuroda, and M. A. A. Franco, Solid State Chem. **17**, 425 (1976).

[32] G. K. Wertheim, Z. Phys. B: Condens. Matter **66**, 53 (1987).

[33] H. J. Freund, Angew. Chem. Int. Ed. Engl. **36**, 452 (1997).

[34] J. Biener, M. Bäumer, R. J. Madix, P. Liu, E. J. Nelson, T. Kendelewicz, and G. E. Brown, Jr., Surf. Sci. **441**, 1 (1999).